Available online at www.sciencedirect.com
SCIENCE DIRECT®
Journal of Sound and Vibration 286 (2005) 745–761
JOURNAL OF SOUND AND VIBRATION
www.elsevier.com/locate/jsvi

Flapwise bending vibration analysis of rotating multi-layered composite beams

Hong Hee Yoo*, Seung Hyun Lee, Sang Ha Shin

School of Mechanical Engineering, Hanyang University, 17 Haengdang-Dong Sungdong-Gu, Seoul 133-791, South Korea

Received 1 April 2004; received in revised form 30 July 2004; accepted 17 October 2004
Available online 23 December 2004

Abstract

A modeling method for the flapwise bending vibration analysis of a rotating multi-layered composite beam is presented in this paper. For the modeling method, the shear and the rotary inertia effects are considered based on Timoshenko beam theory and hybrid deformation variables are employed to derive the equations of motion. Dimensionless parameters are identified from the equations of motion and the combined effects of the dimensionless parameters on the modal characteristics of the rotating composite beams are investigated through numerical study.
© 2004 Elsevier Ltd. All rights reserved.

1. Introduction

Rotating composite beam structures are often found in engineering examples like helicopter blades. In order to design such structures, their modal characteristics need to be estimated accurately. The modal characteristics of rotating flexible structures differ significantly from those of non-rotating flexible structures. Centrifugal inertia force due to rotational motion causes the variation of bending stiffness, which naturally results in the variations of natural frequencies and mode shapes. Since composite structures possess the property of high strength/weight ratio, they are frequently utilized for practical structural designs these days. Moreover, the stiffness property of composite structures can be easily modulated through changing their fiber orientation angles

*Corresponding author. Tel.: +82 2 2290 0446; fax: +82 2 2293 0570.
E-mail addresses: hhyoo@hanyang.ac.kr (H.H. Yoo), hanbando@ihanyang.ac.kr (S.H. Lee), shshin@ihanyang.ac.kr (S.H. Shin).

0022-460X/$ - see front matter © 2004 Elsevier Ltd. All rights reserved.
doi:10.1016/j.jsv.2004.10.007

and number of layers. However, since composite structures usually possess extremely low shear modulus compared to extensional modulus (for instance, the ratio for graphite–epoxy is around $\frac{1}{30}-\frac{1}{50}$), deliberate consideration of shear (even if the composite structure has a slender shape) is usually necessitated to calculate the modal characteristics accurately. For isotropic structures having slender shapes, the shear effect (along with the rotary inertia effect) can be ignored without significant loss of accuracy.

There exists large amount of literature related to modal characteristics of rotating flexible structures. Southwell and Gough [1] pioneered to provide an analytical model (which is often called the Southwell equation) to calculate the natural frequencies of rotating beams. Due to the simplicity of the model, it is still used by many engineers in the field of turbo-machine blade designs. Later, Schilhansl [2] derived the equations of motion for rotating cantilever beams and obtained more accurate coefficients for the Southwell equation based on the Ritz method. Thus, analytical models were introduced in the early stage of research for rotating flexible structures. As the computational technology progressed, a large number of papers in which numerical methods were employed were published (see, for instance, Refs. [3–10]). These papers, however, deal with rotating flexible structures made of isotropic materials. Even if the modal characteristics of stationary composite structures were frequently studied (see, for instance, Refs. [11–15]), relatively a few number of papers regarding rotating composite structures can be found in the literature. In these papers (see, for instance, Refs. [16,17]), nonlinear strain measures were employed to capture the stiffening effect of rotating composite structures. Steady-state in-plane strain measures were obtained from longitudinal equations, and then substituted into bending equations. This two-step procedure is quite involved and lacks rigorousness. Moreover, the combined effects of angular speed, hub radius, slenderness ratio, shear/extension modulus ratio, and fiber orientation angles on the modal characteristics were not scrutinizingly investigated in these works.

The purpose of the present study is to propose a modeling method to analyze the modal characteristics of rotating multi-layered composite beams. The modeling method employs Timoshenko beam theory and hybrid deformation variables to derive the equations of motion. The complexities involved in employing nonlinear strain measures could be avoided in this modeling method. Incidentally, to eliminate the coupling effect between two bending motions (thus, to avoid undesired twist), a set of skew-symmetric fiber orientation angles is employed for the layers. Thus, complexities involved in considering the coupling effect between two bending motions could be avoided with the modeling method and the combined effects of angular speed, hub radius, slenderness ratio, shear/extension modulus ratio, and fiber orientation angles of layers on the modal characteristics are investigated. Especially, the effects of shear and rotary inertia on the modeling accuracy of rotating composite beams are investigated. Such effects are often ignored indiscriminately for slender beams. In the present study, the combined effects of slenderness and shear/extension modulus ratios on the shear and the rotary inertia (thus, on the modal characteristics) of multi-layered composite beams are scrutinizingly analyzed.

2. Derivation of the equations of motion

The configuration of a cantilever beam attached to a rotating rigid hub having radius r is shown in Fig. 1. The elastic deformation of the beam is denoted as $\vec{u}$ in the figure. Conventionally,

Cartesian deformation variables are employed to represent the elastic deformation. In the present study, however, a non-Cartesian variable s denoting arc-length stretch is employed instead of u which denotes the axial deformation. Thus, a hybrid set (Cartesian variable w denoting flapwise bending deformation along with the non-Cartesian variable s) is employed to derive the equations of motion.

The elastic strain energy of a composite beam employing the hybrid set (based on Timoshenko beam theory) is given as follows:

$$U = \frac{1}{2}\int_0^L \left[A_{11}\left(\frac{\partial s}{\partial x}\right)^2 + 2B_{11}\left(\frac{\partial s}{\partial x}\right)\left(\frac{\partial \theta}{\partial x}\right) + D_{11}\left(\frac{\partial \theta}{\partial x}\right)^2 + kA_{33}\left(\theta + \frac{\partial w}{\partial x}\right)^2 \right] \mathrm{d}x \tag{1}$$

where L denotes the length of the beam, k denotes the shear correction factor and θ denotes cross-section rotation angle. Also, A_{ij}, B_{ij} and D_{ij} can be obtained by integrating the properties of the composite beam layers (shown in Fig. 2) as follows:

$$A_{11} = b\int_{-h/2}^{h/2} Q_{11}^{(k)}\,\mathrm{d}z = b\sum_{k=1}^{N} Q_{11}^{(k)}(z_k - z_{k-1})$$

$$A_{33} = b\int_{-h/2}^{h/2} Q_{33}^{(k)}\,\mathrm{d}z = b\sum_{k=1}^{N} Q_{33}^{(k)}(z_k - z_{k-1})$$

$$B_{11} = b\int_{-h/2}^{h/2} Q_{11}^{(k)} z\,\mathrm{d}z = \frac{b}{2}\sum_{k=1}^{N} Q_{11}^{(k)}(z_k^2 - z_{k-1}^2)$$

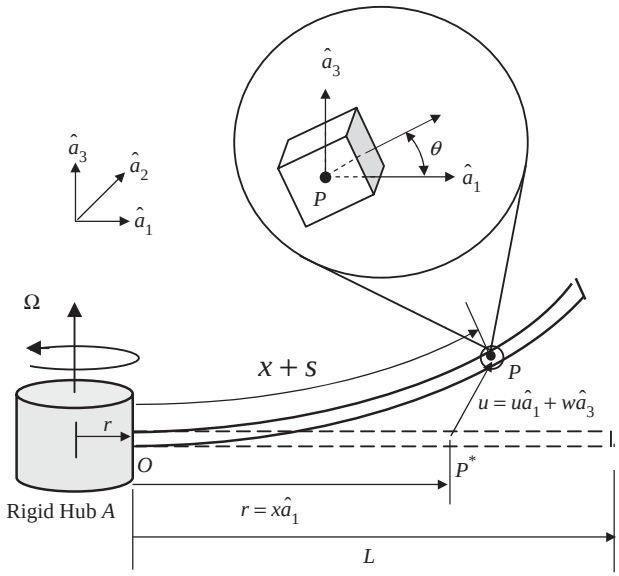

Fig. 1. Configuration of a rotating cantilever beam.

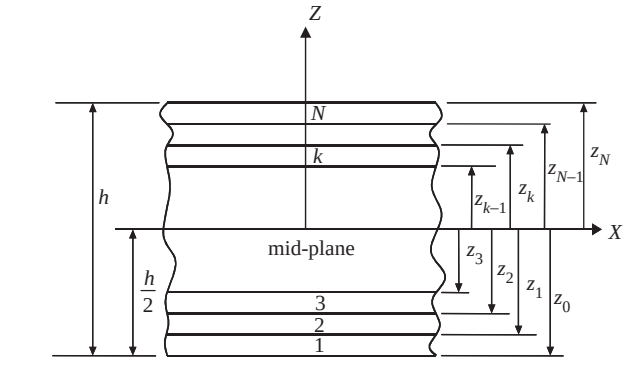

(a) layer numbering and geometry

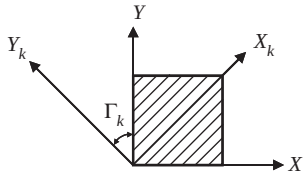

(b) fiber orientation angle of the k-th layer

Fig. 2. Composition of a multi-layered composite beam.

$$D_{11} = b\int_{-h/2}^{h/2} Q_{11}^{(k)} z^2\,\mathrm{d}z = \frac{b}{3}\sum_{k=1}^{N} Q_{11}^{(k)}(z_k^3 - z_{k-1}^3) \tag{2}$$

where z_k and z_{k-1} denote distances from the mid-plane to the top and the bottom surfaces of the kth layer, b and h denote the width and the thickness of the beam, N denotes the number of total layers, and $Q_{ij}^{(k)}$ denotes the off-axis stiffness of the kth layer, which are determined by the fiber orientation angle Γ_k as follows:

$$Q_{11}^{(k)} = C_{11}\cos^4\Gamma_k + C_{22}\sin^4\Gamma_k + 4C_{12}\sin^2\Gamma_k\cos^2\Gamma_k$$

$$Q_{33}^{(k)} = C_{23}\sin^2\Gamma_k + C_{13}\cos^2\Gamma_k \tag{3}$$

where C_{ij}'s are determined by the material properties (see Ref. [18]) as follows:

$$C_{11} = \frac{E_1}{1 - \nu_{13}\nu_{31}}$$

$$C_{22} = \frac{E_2}{1 - \nu_{13}\nu_{31}}$$

$$C_{12} = G_{12}$$

$$C_{23} = G_{23}$$

$$C_{13} = G_{13} \tag{4}$$

where E_i's denote the Young's modulus and G_{ij}'s denote the shear modulus of the composite beam.

If the shear deformation is ignored, $\theta = -\partial w/\partial x$ and the strain energy based on Euler–Bernoulli beam theory is reduced to

$$U = \frac{1}{2}\int_0^L \left[A_{11}\left(\frac{\partial s}{\partial x}\right)^2 - 2B_{11}\left(\frac{\partial s}{\partial x}\right)\left(\frac{\partial^2 w}{\partial x^2}\right) + D_{11}\left(\frac{\partial^2 w}{\partial x^2}\right)^2 \right] \mathrm{d}x \tag{5}$$

To obtain ordinary differential equations of motion, deformation variables are approximated using the Rayleigh–Ritz assumed mode method as follows:

$$s(x,t) = \sum_{j=1}^{\mu_1} \phi_{1j}(x) q_{1j}(t)$$

$$w(x,t) = \sum_{j=1}^{\mu_2} \phi_{2j}(x) q_{2j}(t)$$

$$\theta(x,t) = \sum_{j=1}^{\mu_3} \phi_{3j}(x) q_{3j}(t) \tag{6}$$

where ϕ_{1j}, ϕ_{2j}, and ϕ_{3j} denote spatial mode functions. Any compact set of admissible functions that satisfy the geometric boundary conditions of the beam can be employed as the mode functions. Also, q_{1j}, q_{2j}, and q_{3j} denote generalized coordinates; and μ_1, μ_2, and μ_3 denote the number of the generalized coordinates q_{1j}, q_{2j}, and q_{3j}, respectively.

If the Kane's method (see Ref. [19]) is employed, the equations of motion can be expressed as follows:

$$F_i + F_i^* = 0 \quad (i = 1, \ldots, \mu) \tag{7}$$

where μ is the total sum of μ_1, μ_2, and μ_3; and the generalized forces F_i and F_i^* can be expressed as follows:

$$F_i = -\frac{\partial U}{\partial q_i}$$

$$F_i^* = -\int_0^L \rho\, \vec{v}_i^P \cdot \vec{a}^P \,\mathrm{d}x - \int_0^L \vec{\omega}_i^{\mathrm{dB}} \cdot \left(\vec{\alpha}^{\mathrm{dB}} \cdot \overleftrightarrow{I} + \vec{\omega}^{\mathrm{dB}} \times \overleftrightarrow{I} \cdot \vec{\omega}^{\mathrm{dB}} \right) \mathrm{d}x \tag{8}$$

where q_i's consist of q_{1j}'s, q_{2j}'s, and q_{3j}'s; ρ denotes the mass per unit length of the beam; $\vec{v}_i^P$ and $\vec{a}^P$ denote the partial velocity and the acceleration of the generic point P; $\vec{\omega}^{\mathrm{dB}}$, $\vec{\omega}_i^{\mathrm{dB}}$, and $\vec{\alpha}^{\mathrm{dB}}$, respectively, denote the angular velocity, the partial angular velocity, and the angular acceleration of the arbitrary cross-section of the beam; and $\overleftrightarrow{I}$ denotes the inertia dyadic per beam length.

The velocity of the generic point P can be derived employing the following equation:

$$\vec{v}^P = \vec{v}^O + {}^A\vec{v}^P + \vec{\omega}^A \times (\vec{r} + \vec{u}) \tag{9}$$

where $\vec{v}^O$ denotes the velocity of the reference point O that is fixed to the rigid frame A; ${}^A\vec{v}^P$ denotes the relative velocity of P with respect to A; $\vec{\omega}^A$ is the angular velocity of the rigid frame A; and $\vec{r}$ denotes the position vector from point O to point P in the un-deformed configuration. When the rigid hub rotates at a constant angular speed Ω, each vectors in Eq. (9) can be expressed as follows:

$$\vec{v}^O = r\Omega\hat{a}_2 \tag{10}$$

$${}^A\vec{v}^P = \dot{u}\hat{a}_1 + \dot{w}\hat{a}_3 \tag{11}$$

$$\vec{\omega}^A = \Omega\hat{a}_3 \tag{12}$$

$$\vec{r} = x\hat{a}_1 \tag{13}$$

$$\vec{u} = u\hat{a}_1 + w\hat{a}_3 \tag{14}$$

where $\hat{a}_1$, $\hat{a}_2$, and $\hat{a}_3$ denote mutually orthogonal unit vectors fixed in A. By substituting Eqs. (10)–(14) into Eq. (9), the velocity of the point P can be obtained as follows:

$$\vec{v}^P = \dot{u}\hat{a}_1 + [\Omega(r + x + u)]\hat{a}_2 + \dot{w}\hat{a}_3 \tag{15}$$

In Eq. (15), u and $\dot{u}$ need be expressed in terms of s, w, and their time derivatives (since s instead of u is approximated). The geometric relation between the arc-length stretch s and the Cartesian variables is given as follows:

$$s = u + \frac{1}{2}\int_0^x \left(\frac{\partial w}{\partial \sigma}\right)^2 \mathrm{d}\sigma + (\text{Higher degree terms}) \tag{16}$$

Differentiation of the above equation with respect to time gives

$$\dot{s} = \dot{u} + \int_0^x \left(\frac{\partial w}{\partial \sigma}\right)\left(\frac{\partial \dot{w}}{\partial \sigma}\right)\mathrm{d}\sigma + (\text{Higher degree terms}) \tag{17}$$

Using Eqs. (15)–(17), the partial derivative of the velocity of P with respect to the generalized speed $\dot{q}_i$ can be obtained as follows:

$$\frac{\partial \vec{v}^P}{\partial \dot{q}_i} = \left[\phi_{1i} - \sum_{j=1}^{\mu}\left(\int_0^x \phi_{2i,\eta}\phi_{2j,\eta}\,\mathrm{d}\eta\right)q_j\right]\hat{a}_1 + \phi_{2i}\hat{a}_3 \tag{18}$$

where the subscript η after comma denotes a partial differentiation with respect to the variable. By differentiating Eq. (15) with respect to time, the acceleration of P can be obtained as follows:

$$\vec{a}^P = [\ddot{u} - \Omega^2(r + x + u)]\hat{a}_1 + 2\Omega\dot{u}\hat{a}_2 + \ddot{w}\hat{a}_3 \tag{19}$$

In Eq. (8), the angular velocity, the angular acceleration, and the inertia dyadic per beam length can be obtained as follows:

$$\vec{\omega}^{\mathrm{dB}} = \vec{\omega}^A + {}^A\vec{\omega}^{\mathrm{dB}} = -\dot{\theta}\hat{a}_2 + \Omega\hat{a}_3$$

$$\vec{\alpha}^{\mathrm{dB}} = \Omega\dot{\theta}\hat{a}_1 - \ddot{\theta}\hat{a}_2$$

$$\overleftrightarrow{I} = \rho \frac{I_2}{A} \hat{a}_2 \hat{a}_2 \tag{20}$$

where I_2 denotes the area moment of inertia in $\hat{a}_2$ axis and A is the cross-section area of beam. The partial derivative of the angular velocity with respect to the generalized speed $\dot{q}_i$ can be obtained as follows:

$$\frac{\partial \vec{\omega}^{\mathrm{dB}}}{\partial \dot{q}_i} = -\phi_{3i} \hat{a}_2 \tag{21}$$

Substituting Eqs. (18)–(21) into Eq. (8), the final equations of motion can be obtained. The equations of motion consist of three parts that are related to stretching, flapwise bending, and shear deformations. Since the natural frequencies related to stretching modes are much larger than those of bending modes, only the following equations (that are related to flapwise bending and shear deformations) will be employed for the modal analysis.

$$\sum_{j=1}^{\mu_2} \left(\int_0^L \rho \phi_{2i} \phi_{2j} \, \mathrm{d}x \right) \ddot{q}_{2j} + \sum_{j=1}^{\mu_2} \left(\int_0^L k A_{33} \phi_{2i,x} \phi_{2j,x} \, \mathrm{d}x \right) q_{2j} + \sum_{j=1}^{\mu_3} \left(\int_0^L k A_{33} \phi_{2i,x} \phi_{3j} \, \mathrm{d}x \right) q_{3j} + \Omega^2 \sum_{j=1}^{\mu_2} \left\{ r\rho \left[\int_0^L (L-x) \phi'_{2i} \phi'_{2j} \, \mathrm{d}x \right] q_{2j} + \frac{1}{2} \rho \left[\int_0^L (L^2 - x^2) \phi'_{2i} \phi'_{2j} \, \mathrm{d}x \right] q_{2j} \right\} = 0$$

$$i = 1, \ldots, \mu_2 \tag{22}$$

$$\sum_{j=1}^{\mu_3} \left(\int_0^L \rho \frac{I_2}{A} \phi_{3i} \phi_{3j} \, \mathrm{d}x \right) \ddot{q}_{3j} + \sum_{j=1}^{\mu_2} \left(\int_0^L k A_{33} \phi_{3i} \phi_{2j,x} \, \mathrm{d}x \right) q_{2j} + \sum_{j=1}^{\mu_3} \left(\int_0^L D_{11} \phi_{3i,x} \phi_{3j,x} \, \mathrm{d}x \right) q_{3j} + \sum_{j=1}^{\mu_3} \left(\int_0^L k A_{33} \phi_{3i} \phi_{3j} \, \mathrm{d}x \right) q_{3j} = 0 \quad i = 1, \ldots, \mu_3 \tag{23}$$

Also, the equations of motion based on Euler beam theory are reduced as follows:

$$\sum_{j=1}^{\mu_2} \left(\int_0^L \rho \phi_{2i} \phi_{2j} \, \mathrm{d}x \right) \ddot{q}_{2j} + \sum_{j}^{\mu_2} \left(\int_0^L D_{11} \phi_{2i,xx} \phi_{2j,xx} \, \mathrm{d}x \right) q_{2j} + \sum_{j=1}^{\mu_2} \Omega^2 \left[r \left(\int_0^L \rho (L-x) \phi_{2i,x} \phi_{2j,x} \, \mathrm{d}x \right) q_{2j} + \left(\int_0^L \frac{1}{2} \rho (L^2 - x^2) \phi_{2i,x} \phi_{2j,x} \, \mathrm{d}x \right) q_{2j} \right] = 0$$

$$i = 1, \ldots, \mu_2 \tag{24}$$

To convert the equations of motion into a dimensionless form, the following dimensionless variables are introduced:

$$\tau \equiv \frac{t}{T}, \quad \xi \equiv \frac{x}{L}, \quad \theta_{2i} = \frac{q_{2i}}{L}, \quad \theta_{3i} = q_{3i}, \quad \phi_{ai}(x) = \psi_{ai}(\xi), \quad \gamma = T\Omega \tag{25}$$

The notation T denotes a reference time, which is defined as follows:

$$T \equiv \sqrt{\frac{\rho L^4}{D}} \tag{26}$$

where D denotes the value of D_{11} when all the angles of layers are zero. Introducing the dimensionless variables into Eq. (18), the following equations can be obtained:

$$\sum_{j=1}^{\mu_2} [M_{ij}^{22}\ddot{\theta}_{2j} + \{\beta\alpha^2 K_{ij}^{22} + \gamma^2 K_{ij}^{G2}\}\theta_{2j}] + \beta\alpha^2 \sum_{j=1}^{\mu_3} K_{ij}^{C23}\theta_{3j} = 0 \quad i = 1, \ldots, \mu_2$$

$$\sum_{j=1}^{\mu_3} [M_{ij}^{33}\ddot{\theta}_{3j} + \{\alpha^2\delta K_{ij}^{33} + \beta\alpha^4 M_{ij}^{33}\}\theta_{3j}] + \beta\alpha^4 \sum_{j=1}^{\mu_2} K_{ij}^{C32}\theta_{2j} = 0 \quad i = 1, \ldots, \mu_3 \tag{27}$$

where double dots over the symbol θ_{aj} denotes the double differentiation of θ_{aj} with respect to τ (dimensionless time) and

$$\alpha = \sqrt{\frac{AL^2}{I_2}}, \quad \beta = \frac{(1 - v_{13}v_{31})kA_{33}}{bhE_1}, \quad \delta = \frac{D_{11}}{D} \tag{28}$$

where α denotes the slenderness ratio, β denotes the shear/extension modulus ratio, and δ denotes the bending rigidity modulation ratio, which is determined by the fiber orientation angles Γ_k's. Also the mass and the stiffness indices in Eq. (27) are defined as follows:

$$M_{ij}^{ab} = \int_0^1 \psi_{ai}\psi_{bj}\,\mathrm{d}\xi$$

$$K_{ij}^{ab} = \int_0^1 \psi_{ai,\xi}\psi_{bj,\xi}\,\mathrm{d}\xi$$

$$K_{ij}^{G2} = \int_0^1 \sigma(1-\xi)\psi_{2i,\xi}\psi_{2j,\xi}\,\mathrm{d}\xi + \frac{1}{2}\int_0^1 (1-\xi^2)\psi_{2i,\xi}\psi_{2j,\xi}\,\mathrm{d}\xi$$

$$K_{ij}^{Cab} = \int_0^1 \psi_{ai,\xi}\psi_{bj}\,\mathrm{d}\xi \tag{29}$$

where

$$\sigma = \frac{r}{L} \tag{30}$$

The notation σ denotes the hub radius ratio. If θ_{aj}'s are harmonic functions of τ, the column matrix χ which has θ_{2j} and θ_{3j} as its elements can be expressed as follows:

$$\chi = \mathrm{e}^{\mathrm{j}\omega\tau}\Theta \tag{31}$$

where j denotes imaginary number, ω denotes dimensionless natural frequencies (natural frequencies multiplied by T); and Θ denotes the constant column matrix characterizing the

deflection shape of synchronous motion. Using Eq. (31), Eq. (27) can be expressed as follows:

$$\omega^2 M\Theta = K\Theta \tag{32}$$

where M and K denote square matrices which are constituted as follows:

$$M = \begin{bmatrix} M^{22} & 0 \\ 0 & M^{33} \end{bmatrix}, \quad K = \begin{bmatrix} K_{22} & K_{23} \\ K_{32} & K_{33} \end{bmatrix} \tag{33}$$

The element matrices in Eq. (33) are defined as follows:

$$K_{22} = \beta\alpha^2 K^{22} + \gamma^2 K^{G2}$$

$$K_{23} = \beta\alpha^2 K^{C23}$$

$$K_{32} = \beta\alpha^4 K^{C32}$$

$$K_{33} = \delta\alpha^2 K^{33} + \beta\alpha^4 M^{33} \tag{34}$$

3. Numerical results

In this section, the eigen analysis results obtained by employing Eq. (32) will be presented and discussed. To obtain the numerical results, the composite beams that consist of 4 skew symmetric fiber orientation layers $[0^\circ/\Gamma/-\Gamma/0^\circ]$ are considered. Every layer thickness is identical and the composite beams are made of a graphite–epoxy. The material properties of the graphite–epoxy are given in Table 1.

To check the accuracy of the modeling method proposed in this study, the numerical results obtained by using the proposed modeling method are compared to those presented in Refs. [13,14] and those obtained by a commercial program. For the skew symmetric 4-layer disposition, $\Gamma = 90^\circ$ is employed. The hub radius ratio σ and the slenderness ratio α are given as 0 and 50, respectively. Tables 2 and 3, respectively, show the lowest five dimensionless natural frequencies of the stationary and the rotating composite beams. Table 2 clearly shows that the results obtained by the present modeling method are in good agreement with those of

Table 1
Material properties of the graphite–epoxy used for the composite beams

Notation	Description	Data
E_1	Young's modulus along the fiber direction	14.5×10^{10} Pa
E_2	Young's modulus transverse to the fiber direction	0.96×10^{10} Pa
E_3	Young's modulus transverse to the fiber direction	0.96×10^{10} Pa
G_{12}	Shear modulus between 1 and 2 directions	0.41×10^{10} Pa
G_{13}	Shear modulus between 1 and 3 directions	0.41×10^{10} Pa
G_{23}	Shear modulus between 2 and 3 directions	0.34×10^{10} Pa
v_{13}	Poison's ratio between 1 and 3 directions	0.3
k	Shear correction factor	5/6

Table 2
Comparison of lowest five dimensionless natural frequencies for a stationary composite beam

Mode	Ref. [13]	Ref. [14]	Present
1	3.045	3.073	3.064
2	13.90	14.44	14.36
3	31.46	31.75	31.40
4	48.63	49.68	48.87
5	65.85	66.23	66.24

$\Gamma = 90^\circ$, $\alpha = 50$.

Table 3
Comparison of lowest five dimensionless natural frequencies for the rotating composite beam

γ	Mode	Present	ANSYS	Error (%)
0	1	3.067	3.06	−0.225
	2	14.359	14.172	−1.319
	3	31.397	30.878	−1.681
10	1	10.698	10.63	−0.634
	2	28.802	28.525	−0.972
	3	52.397	51.729	−1.292
50	1	20.522	20.356	−0.815
	2	51.492	51.05	−0.865
	3	86.791	85.786	−1.172

$\Gamma = 90^\circ$, $\alpha = 50$, $\sigma = 0$.

Refs. [13,14] for the stationary beams. Table 3 also shows that the results obtained by the present modeling method are in good agreement with those of a commercial program for rotating beams.

The lowest three dimensionless natural frequencies of a rotating composite beam versus the dimensionless angular speed are shown in Fig. 3. The slenderness ratio $\alpha = 70$ ($L/h \geqslant 20$) and the hub radius ratio $\sigma = 0$ are employed and $\Gamma = 90^\circ$ is employed for the skew symmetric 4-layer disposition. As inspected, all the natural frequencies increase as the angular speed increases. It should be noticed that the second and the third natural frequencies estimated by Euler beam theory are quite different from those estimated by Timoshenko beam theory. If the slender beam were made of an isotropic material (instead of the composite material), the two theories would provide trivial difference.

The variations of the lowest three dimensionless natural frequencies versus the slenderness ratio α are shown in Fig. 4. The dimensionless angular speed $\gamma = 5$ and the hub radius $\sigma = 0.1$ are employed for the analysis. As the slenderness ratio increases, the difference between results produced by two theories decreases. As shown in the figure, the difference becomes negligible as α approaches 210. As shown in these results, the well-known rule of thumb that the two theories

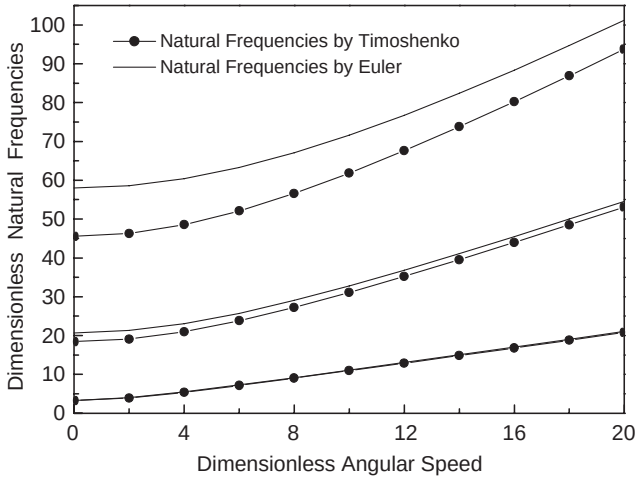

Fig. 3. Lowest three dimensionless natural frequencies versus the dimensionless angular speed obtained by Euler and Timoshenko beam theories.

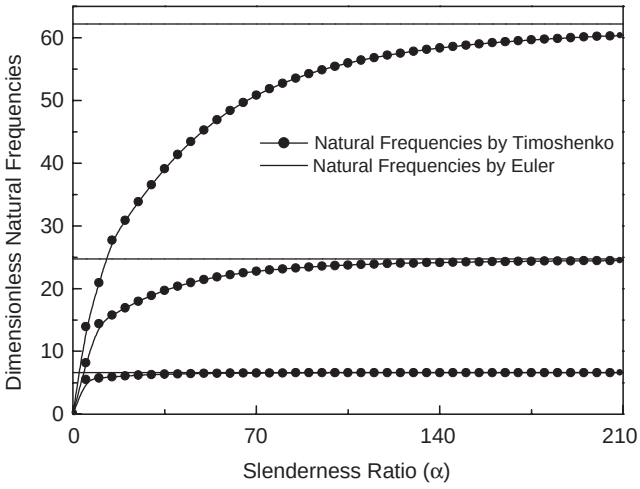

Fig. 4. Lowest three dimensionless natural frequencies versus the slenderness ratio obtained by Euler and Timoshenko beam theories.

produce negligible difference if α exceeds 70 (i.e. $L/h \geqslant 20$) is not valid for composite beams. At $\alpha = 70$, the difference in the produced by the two theories is approximately 8%. Table 4 shows a percentage errors between two results estimated by Euler and Timoshenko beam theories for isotropic and composite beams. The material properties of the composite beams are given in Table 1. $\gamma = 5$ and $\sigma = 0.1$ are employed for the analysis. In the table, λ_i's denote percentage errors between the ith dimensionless natural frequencies estimated by two theories. It is shown that the error gets larger for higher natural frequencies. With an isotropic material, λ_3 becomes less than

Table 4
Percentage errors between two results estimated by Euler and Timoshenko beam theories for isotropic and composite beams

α	λ_1		λ_2		λ_3	
	Iso	Com	Iso	Com	Iso	Com
50	0.311	2.413	5.567	13.30	5.389	27.22
70	0.160	1.340	1.133	8.047	2.898	18.30
100	0.079	0.689	0.562	4.374	1.463	10.84
210	0.018	0.162	0.129	1.079	0.339	2.918

Iso: isotropic, com: composite, $\gamma = 5$, $\sigma = 0.1$.

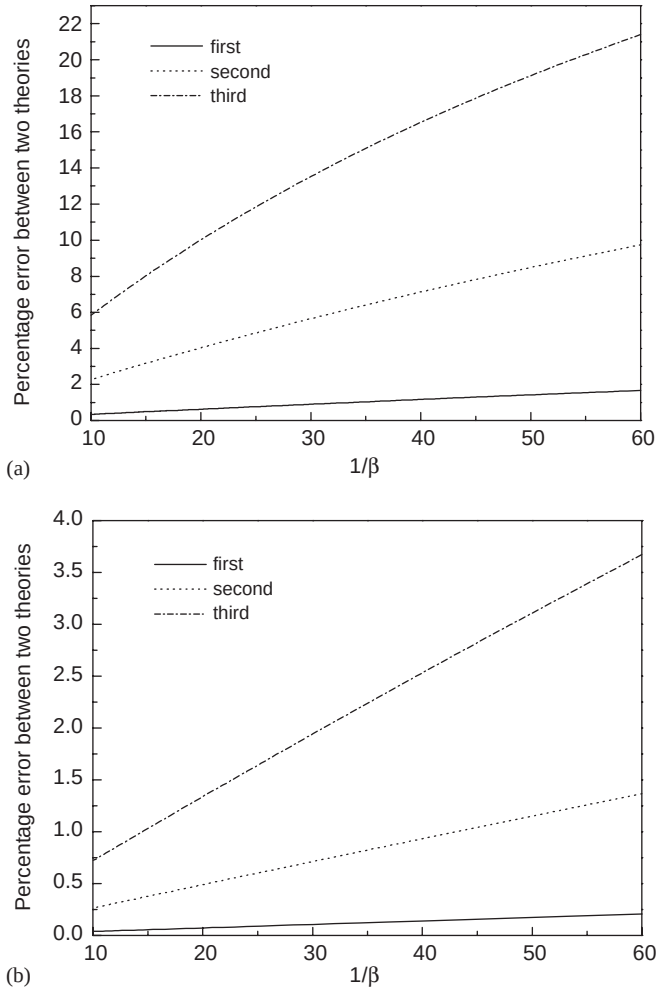

Fig. 5. Percentage error variations versus the inverse of shear/extension modulus ratio. Case of (a) $\alpha = 70$ and (b) $\alpha = 210$.

3% when α exceeds 70. However, for a beam made of the composite material, similar accuracy could be obtained with the Euler beam theory only if α exceeds 210.

The errors estimated for isotropic and composite beams (by Euler and Timoshenko beam theories) are different since the shear/extension modulus ratios for isotropic and composite beams are different. The shear/extension modulus ratio (β) of the composite material is 0.0214 while that of an isotropic material is 0.292. The shear/extension modulus ratio for the composite beam can be calculated by using Eq. (28) and the material properties given in Table 1. The error variations versus the inverse of the shear/extension modulus ratio are shown in Fig. 5. As shown in the figure, the error increases monotonically as the inverse of the shear/extension modulus ratio increases. The slopes of the error loci increase as the mode number increases but they decrease as the slenderness ratio increases.

The variations of the lowest three dimensionless natural frequencies versus the angular speed γ are shown in Fig. 6. The slenderness ratio $\alpha = 70$ is employed. Three hub radius ratios ($\sigma = 0$, 0.5, 2) are employed for the analysis. As shown in the figure, the slopes of the dimensionless frequency loci increase as the hub radius ratio increases.

The variations of the lowest three dimensionless natural frequencies versus the fiber orientation angle Γ of the skew symmetric layers are shown in Fig. 7. The slenderness ratio $\alpha = 70$, the dimensionless angular speed $\gamma = 5$, and the hub radius ratio $\sigma = 0.1$ are employed for the analysis. As shown in the figure, the natural frequencies decrease monotonically as the fiber orientation angle increases. Approximately 5% decrement could be obtained with $\Gamma = 90^\circ$. Also it is noted that the natural frequency variation occurs rapidly in the range of $30^\circ \leqslant \Gamma \leqslant 60^\circ$. However, the variation occurs slowly in the range of $60^\circ \leqslant \Gamma \leqslant 90^\circ$.

The differences of the lowest three mode shapes estimated by Euler and Timoshenko beam theories when $\gamma = 5$, $\sigma = 0.1$, $\alpha = 70$ are shown in Fig. 8. The differences between the two theories are noticeable, if not significant. It is noted that the nodal and anti-nodal points estimated by Timoshenko beam theory slightly move to the fixed end of the cantilever beam.

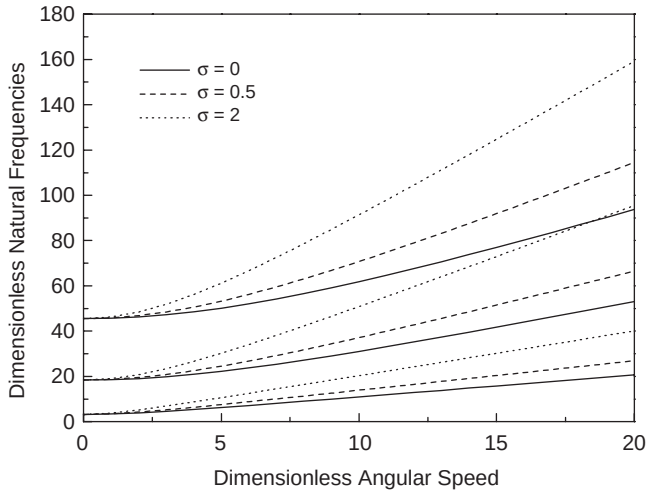

Fig. 6. Lowest three dimensionless natural frequencies versus the dimensionless angular speed and the hub radius ratio.

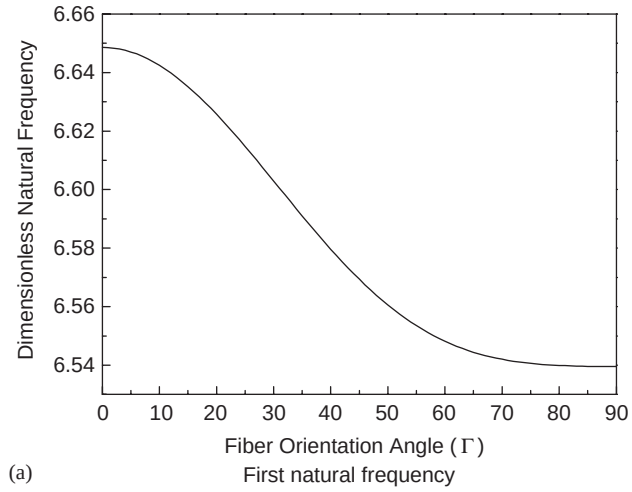

(a) First natural frequency

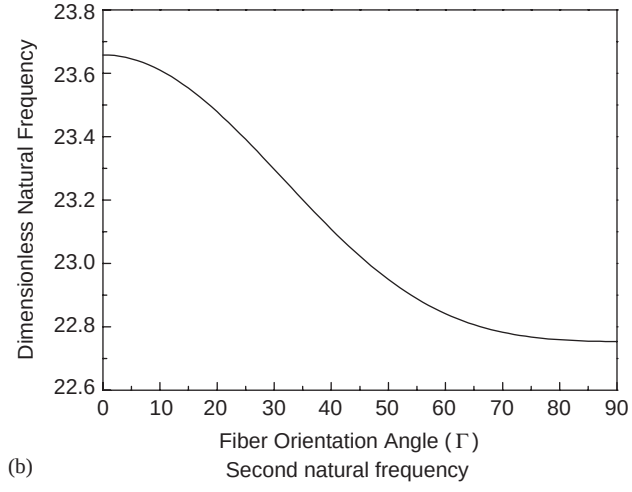

(b) Second natural frequency

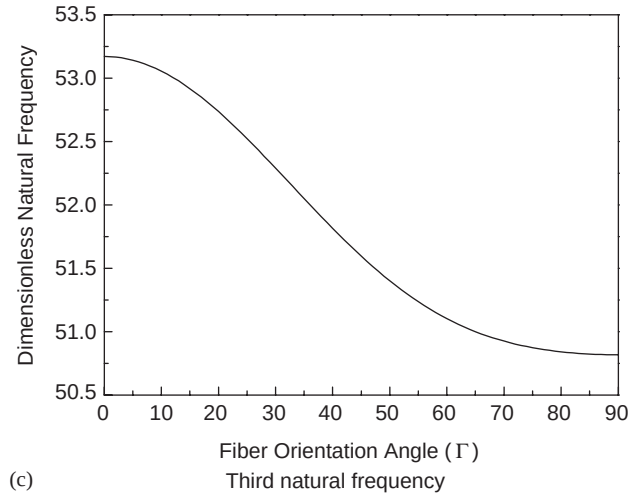

(c) Third natural frequency

Fig. 7. Lowest three dimensionless natural frequencies versus the fiber orientation angle.

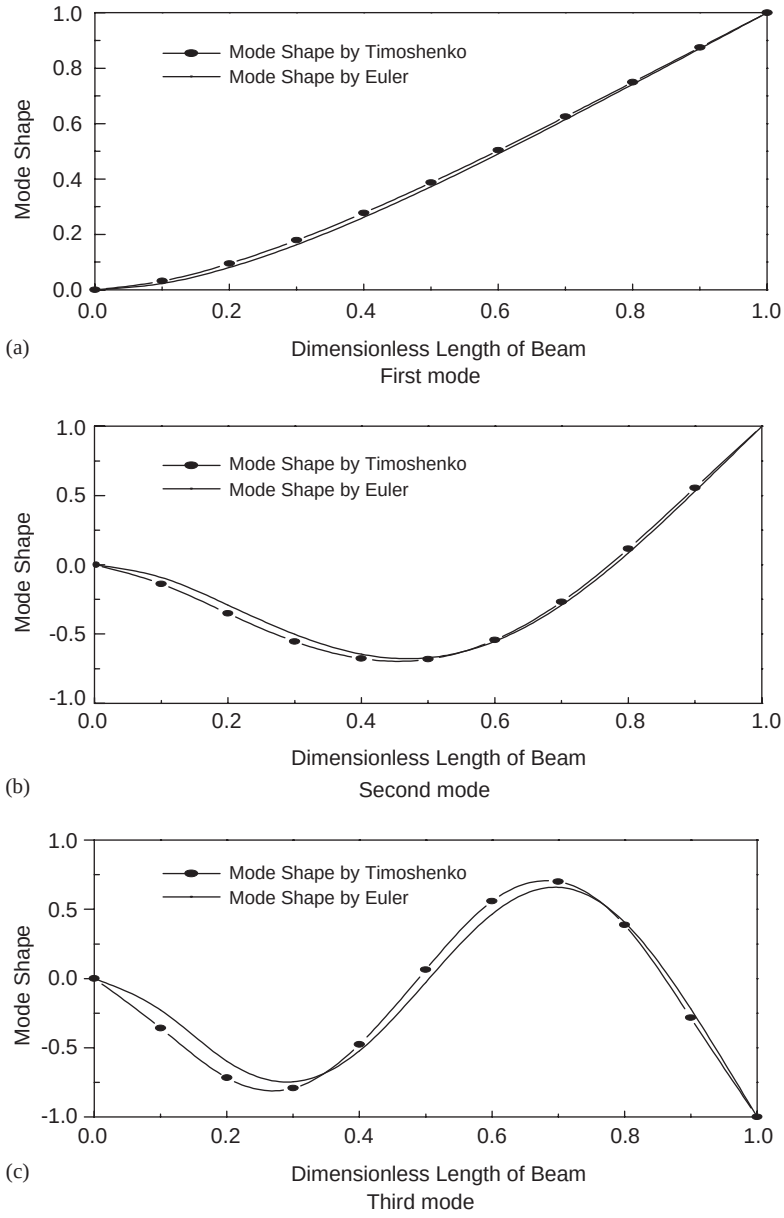

Fig. 8. Variations of the lowest three mode shapes.

4. Conclusion

A modeling method for the flapwise bending vibration analysis of rotating composite beams having skew symmetric layers is presented in this paper. The skew symmetric layers are chosen to avoid the twist deformation caused by the coupling between two bending motions. The Kane's

method along with the Rayleigh–Ritz assumed mode method is employed to derive the equations of motion. The dimensionless parameters are identified from the equations of motion and the effects of the dimensionless parameters on the modal characteristics of the rotating composite beams are investigated. As inspected, the natural frequencies of the rotating composite beams increase as the angular speed increases and the slopes of the natural frequency loci increase as the hub radius ratio increases. The numerical results indicate that the slenderness ratio (to ignore the shear and the rotary inertia effects without losing the accuracy of the modal analysis) should be increased as the shear/extension modulus ratio decreases. It is also found that the natural frequencies can be modulated within approximately 5% by changing the fiber orientation angles of the skew symmetric layers of the composite beam.

Lastly, it should be noted that many coupling effects exist in the deformation of multi-layered composite beams. In the present work, the coupling effect between stretching and flapwise bending motions is only considered so that stiffening effect due to rotational motion can be accurately captured. Other coupling effects are, however, not considered in the present work.

Acknowledgements

This research was supported by Innovative Design Optimization Technology Engineering Research Center through research fund, for which authors are grateful.

References

[1] R. Southwell, F. Gough, The free transverse vibration of airscrew blades, British A. R. C. Reports and Memoranda, No.766, 1921.
[2] M. Schilhansl, Bending frequency of a rotating cantilever beam, *Journal of Applied Mechanics* 25 (1958) 28–30.
[3] S. Putter, H. Manor, Natural frequencies of radial rotating beams, *Journal of Sound and Vibration* 56 (1978) 175–185.
[4] J. Bratt, On impact vibration models for rotating slender beams, *Thin-Walled Structures* 18 (1994) 23–30.
[5] S. Lee, Y. Kuo, Bending frequency of a rotating Timoshenko beam with general elastically restrained root, *Journal of Sound and Vibration* 162 (1993) 243–250.
[6] W. Hsu, A. Shabana, Finite element analysis of impact-induced transverse waves in rotating beams, *Journal of Sound and Vibration* 168 (1993) 355–369.
[7] S. Naguleswaran, Comments on flexural vibration of rotating tapered Timoshenko beams, *Journal of Sound and Vibration* 172 (1994) 559–560.
[8] H. Du, M. Lim, A power series solution for vibration of a rotating Timoshenko beam, *Journal of Sound and Vibration* 175 (1994) 505–523.
[9] M. Al-Ansary, Flexural vibrations of rotating beams considering rotary inertia, *Computers & Structures* 69 (1998) 321–328.
[10] H. Yoo, S. Shin, Vibration analysis of rotating cantilever beams, *Journal of Sound and Vibration* 212 (1998) 807–828.
[11] R. Kapania, S. Raciti, Nonlinear vibration of unsymmetrically laminated beams, *AIAA Journal* 27 (1989) 201–210.
[12] H. Abramovich, Shear deformation and rotary inertia effects of vibrating composite beams, *Composite Structures* 20 (1992) 165–173.
[13] H. Abramovich, A. Livshits, Free vibrations of non-symmetric cross-ply laminated composite beams, *Journal of Sound and Vibration* 176 (1994) 807–828.

[14] M. Singh, A. Abdelnaser, Random response of symmetric cross-ply composite beams with arbitrary boundary conditions, *AIAA Journal* 30 (1992) 201–210.
[15] V. Yildirim, Out-of-plane bending and torsional resonance frequencies and mode shapes of symmetric cross-ply laminated beams including shear deformation and rotary inertia effects, *Communications in Numerical Methods in Engineering* 16 (2000) 67–74.
[16] D. Hodges, Review of composite rotor blade modeling, *AIAA Journal* 28 (1990) 561–565.
[17] S. Nagaraj, Refined structural dynamics model for composite rotor blades, *AIAA Journal* 39 (2001) 339–348.
[18] J. Vinson, T. Chou, *Composite Materials and Their Use in Structures*, Applied Science Publishers Ltd., London, 1975.
[19] T. Kane, D. Levinson, *Dynamics: Theory and Applications*, McGraw-Hill, New York, 1985.